SCIENCE CHINA
Earth Sciences

• RESEARCH PAPER •

doi: 10.1007/s11430-017-9122-x

A climatological northern boundary index for the East Asian summer monsoon and its interannual variability

CHEN Jie[1], HUANG Wei[1*], JIN LiYa[1,2], CHEN JianHui[1], CHEN ShengQian[1] & CHEN FaHu[1,3†]

[1] *Key Laboratory of Western China's Environmental Systems (Ministry of Education), College of Earth and Environmental Sciences, Lanzhou University, Lanzhou 730000, China;*
[2] *School of Atmospheric Sciences, Chengdu University of Information Technology, Chengdu 610225, China;*
[3] *Key Laboratory of Alpine Ecology and Biodiversity (LAEB), Tibetan Plateau Earth Sciences of the Chinese Academy of Sciences, Beijing 100101, China*

Received May 13, 2017; accepted October 9, 2017; published online November 16, 2017

Abstract A long-term perspective on the spatial variation of the northern boundary of the East Asian summer monsoon (EASM) and the related physical mechanisms is important for understanding past climate change in Asia and for predicting future changes. However, most of the meteorological definitions of the EASM northern boundary do not correspond well to the actual geographical environment, which is problematic for paleoclimatic research. Here, we use monthly CMAP and GPCP precipitation data to define a new EASM northern boundary index by using the concept of the global monsoon, which is readily applicable to paleoclimatic research. The results show that the distribution of the 2 mm day^{-1} precipitation isoline (i.e., 300 mm precipitation) has a good relationship with the spatial distribution of modern land cover types, the transitional climate zone and the potential natural vegetation types, in China. The locations of the precipitation isolines also correspond well to the locations of major shifts in wind direction. These results suggest that the 2 mm day^{-1} isoline has a clear physical significance since the climatic, ecological, and geographical boundary can be used as the northern boundary index of the EASM (which we call the climatological northern boundary index). The index depicts the northeast-southwest orientation of the climatological (1981−2010) EASM northern boundary, along the eastern part of the Qilian Mountains-southern foothills of the Helan Mountains-Daqing Mountains-western margin of the Greater Khingan Range, from west to east across Northwest and Northeast China. The interannual change of the EASM northern boundary from 1980 to 2015 covers the central part of Gansu, the northern part of Ningxia, the eastern part of Inner Mongolia and the northeastern region in China. It can extend northward to the border between China and Mongolia and retreat southward to Shangdong-central Henan. There is a 200−700 km fluctuation range of the interannual EASM northern boundaries around the locations of the climatological northern boundary. In addition, the spatial variation of the interannual EASM northern boundaries gradually increases from west to east, whereas the trend of north-south fluctuations maintains a roughly consistent location in different regions.

Keywords East Asian summer monsoon, Climatological northern boundary index, Interannual change, Spatial fluctuations

Citation: Chen J, Huang W, Jin L Y, Chen J H, Chen S Q, Chen F H. 2017. A climatological northern boundary index for the East Asian summer monsoon and its interannual variability. Science China Earth Sciences, 60, doi: 10.1007/s11430-017-9122-x

1. Introduction

Monsoons are an important component of the global atmospheric circulation system and have a direct impact on human life and prosperity across a large area of the world. In classical climatology, a monsoon is a seasonal reversal of the local winds within the ground layer (Ramage, 1971; Webster, 1987). With continuing research, the concept of a monsoon was expanded in the early 21 century from a regional climatic

* Corresponding author (email: whuang@lzu.edu.cn)
† Corresponding author (email: fhchen@itpcas.ac.cn, fhchen@lzu.edu.cn)

phenomenon to a global atmospheric circulation phenomenon with a seasonal wind reversal and alternating wet and dry seasons; e.g., the global monsoon (GM) (Trenberth et al., 2000; Wang and Ding, 2006, 2008). This initiated a new area of monsoon research (Wang, 2009) and subsequently research into the GM area and related precipitation has expanded considerably (Wang and Ding, 2006, 2008; Zhou et al., 2008a; Hsu et al., 2011; Wang et al., 2012; Lin et al., 2014; Wang P X et al., 2014).

The East Asian summer monsoon (EASM) is an important component of the GM system (Wang B et al., 2014). The northern boundary of the GM area can be considered as the northern boundary of the EASM and its spatial fluctuations on interannual and interdecadal scales are caused by changes in the related summer monsoon strength. The zone of fluctuation of the EASM northern boundary has been termed the EASM edge zone (Xu and Qian, 2003; Hu and Qian, 2007). Because the precipitation in the EASM edge zone is less than that in the EASM core area, its response to changes in EASM strength is more sensitive, and the precipitation fluctuations are particularly significant; hence the impact on vegetation, ecology and agriculture is stronger on the EASM edge. It is also a farming-pastoral ecotone, a climatically sensitive zone, and is prone to frequent natural disasters in China (Shi, 1996; Fu, 2003). Most of the northern part of China is located in the EASM edge zone. Study of the changes in the EASM northern boundary not only enables us to fully understand climate change in northern China, but it is also significant for understanding the mutual feedbacks between climate change and the regional ecosystem.

Currently, the definitions of the northern boundary of the EASM can be divided into two categories. One is from the perspective of air masses, where the EASM northern boundary is considered as the zone of interaction between warm and wet air masses in low latitudes and cold and dry air masses in middle and high latitudes. For example, Wang et al. (1999) considered the degree of warmth and humidity of the air masses, and the wind direction, and used pentad mean data to define two criteria for the EASM region: (1) southwest winds exceed 2 m s^{-1}, (2) the potential pseudo-equivalent temperature (θ_{se}) exceeds 340 K to the south of 30°N, and exceeds 335 K to the north of 30°N. The definition of the EASM northern boundary by Wu et al. (2005) is that the pentad mean wind field of southwest and south winds exceeds 3 m s^{-1} at 850 hPa, and the pentad mean θ_{se} exceeds 335 K at 850 hPa. The other category is from the perspective of precipitation, and highlights the important feature that the EASM precipitation advances northward, with seasonal variability. For example, Qian and Lee (2000), based on the strong convective precipitation at the onset of the South China Sea monsoon, defined the northernmost position of the 4 mm day^{-1} pentad mean isochrones as the EASM northern boundary. The region where the difference between the pentad mean precipitation and the precipitation in January exceeds 5 mm day^{-1} is the EASM region, as defined by Wang and Lin (2002). Qian et al. (2007) also used 4 mm day^{-1} isochrones of the 7-day running mean precipitation to delimit the range of variation of the EASM northern boundaries.

In conclusion, there is no uniform standard for defining the EASM northern boundary, and the existing definitions are based on daily or pentad data. Research on the northern boundary of the EASM on longer timescales, and its variability (despite the possibility of obtaining climatic elements on long timescales through numerical simulation) is based on monthly resolution data. In paleoclimatic research, definition of the EASM northern boundary lacks strict criteria and indicators (e.g., Winkler and Wang, 1993; Chen et al., 2008, 2010). Therefore, the existing definitions based on the daily or pentad data cannot be applied to the study of the variability of the paleomonsoon northern boundary, which hinders our understanding of the spatiotemporal variation and mechanisms of the EASM on longer timescales. The region of GM influence is mainly determined by monthly precipitation data (Wang et al., 2012), which is potentially useful for paleomonsoon research (Liu et al., 2009, 2012; Jiang et al., 2015a, 2015b). Based on the concept of the GM, here we define a new EASM northern boundary index by using monthly data, evaluate its reliability, determine the locations of the EASM northern boundaries, and discuss its spatiotemporal variation against the background of ongoing climate change.

2. Data and methods

The two monthly precipitation datasets used in this study were obtained from the Global Precipitation Climatology Centre (GPCC; Huffman et al., 2009) and the Climate Prediction Center (CPC) Merged Analysis of Precipitation (CMAP; Xie and Arkin, 1997). The two datasets cover the period from 1979 to 2015, with a horizontal resolution of 2.5° latitude by 2.5° longitude. They are always used to derive global monsoon features. In addition to integrating the instrumental data, satellite retrieval precipitation data is included, which makes the datasets more accurate. Since for some regions there is inconsistency between the GPCP and CMAP data, an arithmetic mean of the two datasets was used to reduce the uncertainty (Zhou et al., 2008b; Hsu et al., 2011). For a comparative analysis, daily precipitation data were obtained from the Global Precipitation Climatology Center (GPCC) from 1988 to 2013, with a horizontal resolution of 1° latitude by 1° longitude (Schamm et al., 2015), and monthly precipitation data were obtained from the Climate Research Unit, with a horizontal resolution of 0.5° latitude by 0.5° longitude (CRU TS 3.23; Harris et al., 2014). Monthly winds during 1979–2015 at various pressure levels were obtained from the National Center for

Environmental Prediction/National Center for Atmospheric Research (NECP/NCAR), with a horizontal resolution of 2.5° latitude by 2.5° longitude (Kalnay et al., 1996). In addition, two global land-cover-type datasets were downloaded from NASA EARTHDATA websites (see https://daac.ornl.gov/) from the International Satellite Land Surface Climatology Project (ISLSP II). One dataset was generated using a full year of MODerate Resolution Imaging Spectroradiometer (MODIS) data covering the period from October 2000 to October 2001 (Friedl et al., 2010), with a horizontal resolution of 0.25°×0.25°. These products describe the geographic distribution of the 17 land-cover classification scheme proposed by the International Geosphere-Biosphere Programme (IGBP). The other dataset is of potential natural vegetation (PNV) cover which contains 15 major types, representing the global vegetation cover that would most likely now be in equilibrium with present-day climate and natural factors, in the absence of human activity (Ramankutty and Foley, 2010). The horizontal resolution is 0.25°×0.25°.

3. Results and discussion

3.1 Definition of the EASM northern boundary and its spatiotemporal variation

The GM area is defined as the region where the local summer-minus-winter precipitation exceeds 2 mm day^{-1} and the local summer precipitation exceeds 55% of total annual precipitation (Wang et al., 2012). In the Northern Hemisphere, the local summer is defined as May to September, and the local winter is defined as November to March. For the northern region of China, the East Asian winter monsoon (EAWM) is one of the most active circulation systems in the Northern Hemisphere (Chen and Sun, 1999; Huang et al., 2003) and provides favorable weather conditions for cold waves, leading to the frequent impact of cold air and causing severe weather (e.g., freezing rain and snow) in northern China (Guo, 1994; Gu et al., 2008; Wen et al., 2009; Sun et al., 2010; Wang et al., 2011). These severe weather events can also increase the winter precipitation, which decreases the precipitation difference between summer and winter, and thus reducing the accuracy of GM signals. The EASM northern boundary, based on the definition of the GM area, exhibits a large discrepancy with the climatic, ecological and geographical situation, especially in the EASM northern edge zone where the precipitation is relatively low. Clearly, the EASM northern boundary index based on the precipitation difference between summer and winter cannot be applied to the EASM region. Given the characteristic relative high winter precipitation in the EASM region, we suggest that a definition of the EASM northern boundary based on the summer (May–September) isoline is more reliable. The index differs from the definitions for the EASM northern boundary in meteorology and the GM area and therefore it is termed the Climate Northern Boundary Index (CNBI) to distinguish it from other EASM northern boundary indexes.

Here, we focus on the EASM northern boundary in Northeast and Northwest China, because the smaller number of meteorological stations on the Tibetan Plateau (TP) results in a large error in the gridded precipitation data for the region. Summer isolines for 1, 1.5, 2.0 and 2.5 mm day^{-1}, were calculated as annual means from 1980 to 2015 and as a total mean from 1981 to 2010, by using the arithmetic mean of the CMAP and GPCP datasets. The results show that the summer 2.0 mm day^{-1} isoline corresponds well to the climatic, ecological and geographical situation (as we discuss below). The CNBI depicts the northeast-southwest orientation of the climatological EASM northern boundary, along the eastern part of the Qilian Mountains-southern foothills of the Helan Mountains-Daqing Mountains-western margin of the Greater Khingan Range, from west to east in northern China (the red heavy line in Figure 1). The interannual change of the EASM northern boundary covers the central part of Gansu, the northern part of Ningxia, the eastern part of Inner Mongolia and the northeastern region in China (100°E−120°E). There are fluctuations of 200−700 km of the interannual EASM northern boundaries around the locations of the climatic EASM northern boundary. In addition, the northeast-southwest orientation of the spatial fluctuations gradually increases from west to east (black dashed lines in Figure 1). The region close to the margin of the TP and the western part of the Loess Plateau exhibits the smallest spatial variation of the interannual EASM northern boundaries, possibly because of the limitations imposed by the terrain. In some years, the annual EASM northern boundaries exhibit a dry "tongue" extending to the southeast part of Northeast China (115°E−120°E), which results in the largest fluctuation of the interannual EASM northern boundaries in Northeast China.

During the period of 1980−2015, the interannual EASM northern boundaries fluctuated in the northern region of China. To better reflect the fluctuations in different years, latitude-averaged EASM northern boundaries for 100°E−105°E, 105°E−110°E and 110°E−115°E were calculated and are illustrated in Figure 2. The locations of the interannual EASM northern boundaries are generally southerly and the fluctuations of the northern boundaries are smallest in the westernmost region of 100°E−105°E (Figure 2a). In the easternmost region of 110°E−115°E, they are generally northerly and the fluctuations are largest, with the largest fluctuations extending across 8° of latitude (Figure 2c). The changes in the interannual EASM northern boundaries in the three regions share a common feature in that the north-south orientation of the fluctuations was greater before 2000 than subsequently. In addition, the trends of the interannual

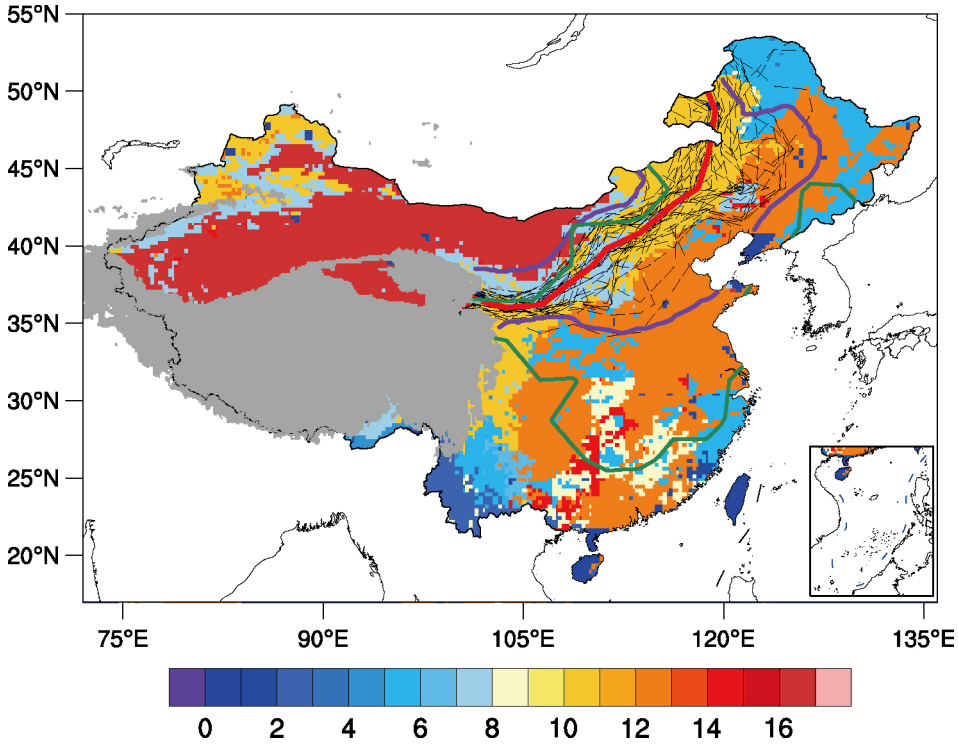

Figure 1 Depiction of the northern boundaries of the East Asian Summer Monsoon (EASM) using the summer (May–September) 2 mm day^{-1} isolines based on the CNBI. The black dashed lines represent the annual locations of the EASM northern boundaries and the red heavy line represents the locations of the climatological EASM northern boundary (1981−2010). The green heavy lines represent the most northerly and southerly locations of the northern boundaries based on the definition of the GM area from 1980 to 2015. The two purple heavy lines are the northern and southern boundaries of the transitional climate zone (Wang et al., 2017). The gray area represents the area of altitude >3000 m and the colored areas represent different modern land cover types based on MODIS satellite data. 0, Water Bodies; 1, Evergreen Needleleaf Forest; 2, Evergreen Broadleaf Forest; 3, Deciduous Needleleaf Forest; 4, Deciduous Broadleaf Forest; 5, Mixed Forest; 6, Closed Shrublands; 7, Open Shrublands; 8, Woody Savannas; 9, Savannas; 10, Grasslands; 11, Permanent Wetlands; 12, Croplands; 13, Urban and Built-Up; 14, Cropland/Natural; 15, Permanent Snow and Ice; 16, Barren or Sparsely Vegetated; 17, Unclassified.

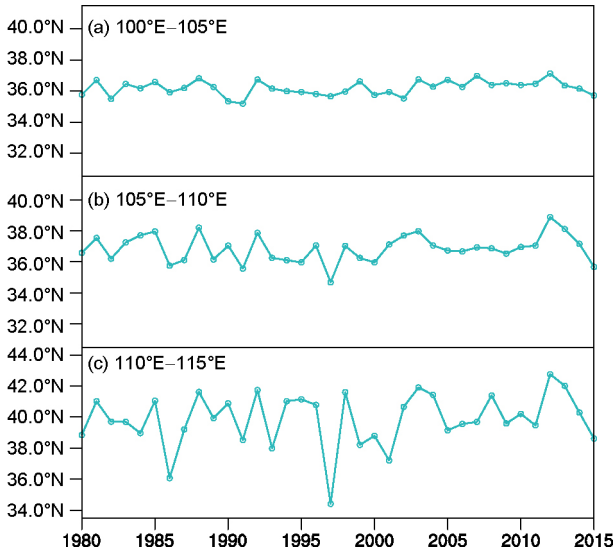

Figure 2 Temporal variations in the annual latitude-averaged EASM northern boundaries for 100°E−105°E (a), 105°E−110°E (b), and 110°E−115°E (c).

EASM northern boundaries in different regions are generally consistent; for example, the annual northern boundary clearly shifted southward in different regions in 1997, corresponding to the weak summer monsoon in that year. The correlation coefficients for the interannual EASM northern boundaries between 100°E−105°E (Figure 2a) and 105°E−110°E (Figure 2b), 110°E−115°E (Figure 2c) are 0.61 and 0.42, respectively. The correlation coefficient for the interannual EASM northern boundaries between 105°E−110°E (Figure 2b) and 110°E−115°E (Figure 2c) is 0.74. All correlation coefficients are significant at the 99% confidence level, demonstrating that the trends of the interannual EASM northern boundaries were almost the same in the region of 100°E−115°E.

3.2 Comparison of the CNBI and other EASM northern boundary indexes

The EASM region based on the definition of the GM area differs from the actual climatic conditions. One reason for this is that there is plentiful precipitation in different seasons in some areas of Southeast China, resulting in the local summer precipitation comprising less than 55% of total annual precipitation; thus, these areas are excluded from the summer monsoon region based on the concept of the GM (Wang B et al., 2014; Jiang et al., 2015). We decided this conclusion,

while consistent with the definition of the index, cannot conflict with the actual climatic conditions in China. In fact, in southeastern China, the land cover types are dominated by croplands and woody savannas (Figure 1) and the climate in summer is affected by southwest winds from the South China Sea (Figure 3); thus, the region is typically influenced by the summer monsoon. This issue indicates that the application of the GM definition to the EASM region is problematic, and the local climate needs to be considered to understand the monsoon within the framework of the GM. The other reason is that the locations of the annual EASM northern boundaries reveal that most of the regions in China are not influenced by the summer monsoon (green heavy lines in Figure 1): using the definition of the GM area to define the EASM region in several extreme years, they are located to the south side of the transitional climate zone (purple heavy lines in Figure 1). Because the impact of the EAWM increases the winter precipitation, the locations of the annual EASM northern boundaries may lie more southerly than the actual climatic conditions from the perspective of the GM.

The CNBI differs from the indexes that focus on the onset, advance and retreat of the EASM by using daily or pentad precipitation data (Qian and Lee, 2000; Wang and Lin, 2002; Jiang et al., 2006; Hu and Qian, 2007; Qian et al., 2007, 2009). Thus, the existing indexes and the CNBI were compared to verify that the definition based on monthly data could accurately depict the locations of the EASM northern boundaries. A widely-used index is the 4 mm day^{-1} isochrones based on a 7-day running mean of precipitation which defines the EASM northern boundary. Evidently, the locations of the climatological EASM northern boundary, based on the 4 mm day^{-1} isochrones, are almost the same as those based on the CNBI, and the locations of the two indexes also have similar characteristics. Both exhibit the northeast-southwest and northward extension of the ridge around 110°E, the ridge corresponding to the diversion of the southerly winds (Figure 3). However, there are several differences in some regions; for example, the locations of the climatological EASM northern boundary defined by Qian et al., (2007) is more southerly than that based on the CNBI in the Qilian Mountains from 100°E−105°E. The locations of the climatological EASM northern boundary based on the CNBI are consistent with the trend of the Qilian Mountains and are in better accord with the actual conditions of atmospheric circulation. In fact, the distribution of precipitation in this region is consistent with the Central China, where there is a typical summer monsoon region in which summer is the major precipitation season. Thus, despite the two definitions having different emphases, the CNBI more accurately depicts the location of the EASM northern boundary. In addition, we used GPCC and CRU datasets to calculate the locations of the climatological EASM northern boundary. The resulting locations correspond well with the results based on the CMAP and GPCP datasets, indicating that the results based on different datasets do not affect the locations of the climatological EASM northern boundary of the CNBI (Figure 3).

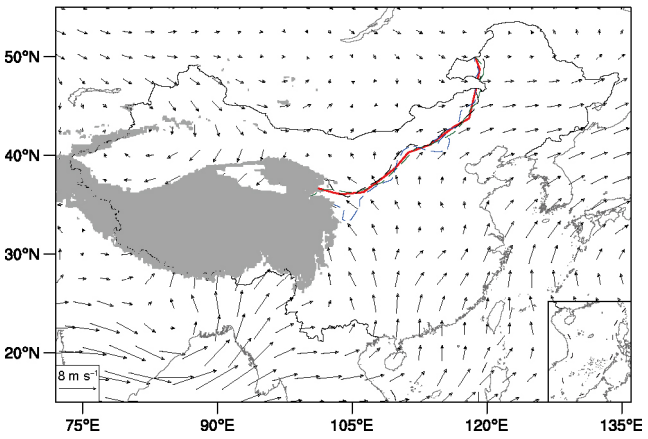

Figure 3 Locations of the EASM northern boundaries (the red line and black and green dashed lines represent the locations of the climatological EASM northern boundary of the CNBI using CMAP and GPCP arithmetic mean data, and GPCC and CRU data, respectively; the blue dashed line shows the climatological northern boundary used the GPCC data according to Qian et al. (2007) and July−August wind vectors at 850 hPa during 1988−2013. The gray area represents the area with altitude >3000 m.

Further comparison of the CNBI with different EASM northern boundary indexes revealed that the location of the climatological EASM northern boundary in northern and northwestern China, based on the CNBI, is similar to that for most of the other indexes (Qian and Lee, 2000; Jiang et al., 2006; Tang et al., 2010; Li et al., 2013). The north-south orientation of the climatological EASM northern boundary based on the CNBI is also similar with the results of Jiang et al. (2006) and Li et al. (2013), but different from those of Qian and Lee (2000) and Tang et al. (2010) for Northeast China; the latter argue that the orientation of the climatological EASM northern boundary is northeast-southwest, consistent with the northeast-southwest distribution of the Greater Khingan Range. However, the 1000−1400 m altitude of the Greater Khingan Range only blocks some of the water vapor transport from the south, and the vegetation type in the northern Greater Khingan Range is mixed forest which requires abundant precipitation. In addition, based on the fact that the EASM precipitation advances northward with seasonal variability, it is evident that EASM precipitation can reach the Greater Khingan Range (Jiang et al., 2006; Qian et al., 2009). Hence, we considered that a north-south orientation of the climatological EASM northern boundary is more reasonable in Northeast China, and that the CNBI is reliable. The orientation of the modern EASM northern boundary, inferred from the perspective of the long timescales typical of paleoclimatic research, is northeast-southwest in Northeast China (Chen et al., 2008, 2010). In conclusion, the CNBI, which uses monthly data, provides a reliable reference for the location of the modern EASM northern boundary for

paleoclimatic research.

3.3 Comparison of the EASM northern boundary and climatic, ecological and geographical divisions

The location of the EASM northern boundary is mainly determined by the southerly summer monsoon circulation. Therefore, we compared the wind distribution during the strongest summer-monsoon months (July−August) and the location of the climatological EASM northern boundary to verify the reliability of the location of the climatological EASM northern boundary of the CNBI (Figure 3). The results reveal that the southerly winds from the Indian Ocean and the Pacific turn to the southeast and southwest around 110°E and then move to Northwest and Northeast China, respectively. Due to the blocking effect of TP and the westerlies, the southeast winds are unable to penetrate deeply into Northwest China, whereas the southwest and west winds converge and form a cyclone in Northeast China. The climatological EASM northern boundary is mainly located near the southeast and southwest winds, because of the southward shift of the southerly winds. The shift of the southerly winds to Northeast China coincides with the northward extension of the northern boundary around 100°E, while the cyclone develops in the northern part of northeast China, supplying more water vapor to the area, and further resulting in the northern boundary being located on the western side of the cyclone. In general, the locations of the climatological EASM northern boundary based on the CNBI are consistent with the spatial variation of atmospheric circulation.

The land cover types in Inner Mongolia are grasslands and woody savannas, Northeast China is dominated by croplands and mixed forest, and Northwest China is barren or sparsely vegetated (Figure 1). The climatological EASM northern boundary is located in the central of grasslands and open shrublands, and in an ecotone (Zhao and Qiu, 2001; Yan et al., 2008). The interannual EASM northern boundaries are mainly located in grasslands and open shrublands and are absent in the sparsely vegetated arid region of Northwest China (Feng and Fu, 2013), and in the well-vegetated summer monsoon core area (Wang and Lin, 2002). The land cover types are mainly affected by climatic conditions, and the fluctuations in the EASM northern boundary generally reflect the spatial distribution of modern land cover types, indicating that the fluctuations of the interannual EASM northern boundaries based on the CNBI reliably reflect the influence of climate on land cover. The work of Feng and Fu (2013) reveals that the fluctuations of the interannual EASM northern boundaries correspond well with the spatial distribution of semi-arid and dry sub-humid areas in China, against the background of global warming (Figure 1). Semi-arid and dry sub-humid areas are designated the "transitional climate zone" (Wang et al., 2017). The spatial variation of the interannual EASM northern boundaries may be an important contributor to climatic instability in the region. There is a broad correspondence between the range of fluctuation of the EASM northern boundary and the transitional climate zone, confirming the reliability of the CNBI.

Increasing economic development and resource consumption are paralleled by significant environmental changes including deforestation and other major vegetation changes, and thus both human activity and natural processes contribute to determine modern land cover types. To further verify the reliability of the CNBI, we selected the dataset of PNV types to eliminate the influence of human activities, and then compared it with the fluctuations of the EASM northern boundary and the transitional climate zone. We found that the interannual spatial fluctuations of the EASM are mainly located in the transitional zone of the PNV transition from forest to dense shrubland (Figure 4), which represents the transitional zone for vegetation under natural conditions. Its ecological environment is fragile and climatically sensitive and thus it is also sensitive to climate change (Fu, 1992). The fluctuations of the interannual EASM northern boundaries correspond more closely to the distribution of PNV types than to the modern land cover types. The distribution of savanna and grassland in Northeast China is more consistent with the location of the dry "tongues" of the annual EASM northern boundaries, and they also coincide well with the southern boundary of the transitional climate zone (Figure 4). This good relationship further demonstrates that the CNBI has significance as an ecological and climatic zone. In summary, from the perspective of both climate and ecology, the CNBI

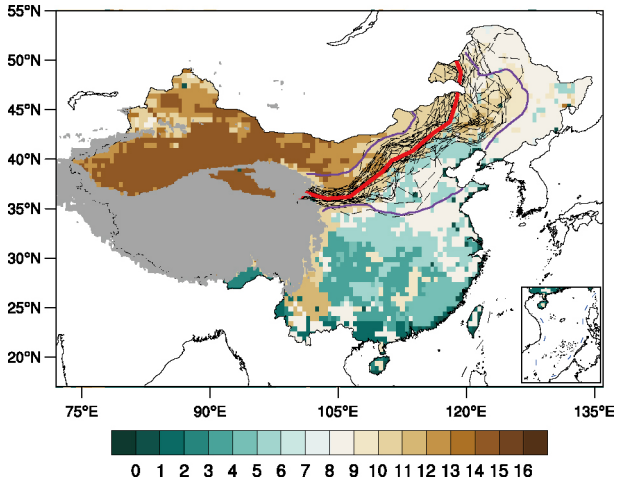

Figure 4 Distribution of potential natural vegetation (PNV) types in China. 0, Water bodies, 1, tropical evergreen forest; 2, tropical deciduous forest; 3, temperate broadleaf evergreen forest; 4, temperate needleleaf evergreen forest; 5, temperate deciduous forest; 6, boreal evergreen forest; 7, boreal deciduous forest; 8, mixed forest; 9, savanna; 10, grassland/steppe; 11, dense shrubland; 12, open shrubland; 13, tundra; 14, desert; 15, polar desert/rock/ice; 16, no data over land. Other details are consistent with Figure 1.

defined in this study accurately portrays the locations of the EASM northern boundaries and their fluctuations, and has a clear significance as a climatic, ecological and geographical boundary.

3.4 Causes of changes in the interannual EASM northern boundary

We found that the interannual EASM northern boundaries in different locations exhibited a similar regular pattern of change. To better understand the physical mechanisms behind this consistency, the years with more than two values exceeding a standard deviation of 0.75 were selected to represent the years with more northerly or southerly locations of the interannual EASM northern boundaries, from Figure 2. For the northerly location, these years are 1988, 1992, 2003, 2012 and 2013; and for the southerly location they are 1982, 1986, 1991, 1997, 2000 and 2015. We then conducted a composite analysis of the wind field at 850 hPa from July to August. In Figure 5a and c, it is evident that the cyclone in the northern part of Northeast China in those years with a more northerly location is more northerly than in the years with a more southerly location, indicating that the summer monsoon transports water vapor further north in northerly-located years. However, the southerly winds and westerly winds converge and form a cyclone in Northeast China, making it difficult to define the boundaries of the westerly- and summer-monsoon-affected areas, which is also noted by other workers (Qian et al., 2009). In addition, the summer monsoon intensity reflects the features of the main part of monsoon, while the locations of the northern boundaries reflect the features of the monsoon edge. Despite the summer monsoon′s ability to transport water vapor further north in northerly-located years (Figure 5a and b), the intensity of the summer monsoon cannot reflect changes in EASM northern boundary locations (Wu et al., 2005; Hu and Qian, 2007). In contrast, the relationship between summer monsoon precipitation in North China and the locations of the EASM northern boundary is clear. The anomalous anticyclonic circulation in the eastern part of China promotes the transport of warm and moist air to northern China, increasing the precipitation in the northern and northeastern parts of China in northerly-located years (Figure 5b). Conversely, when the transport of warm and wet air is reduced, there is decreased precipitation in these

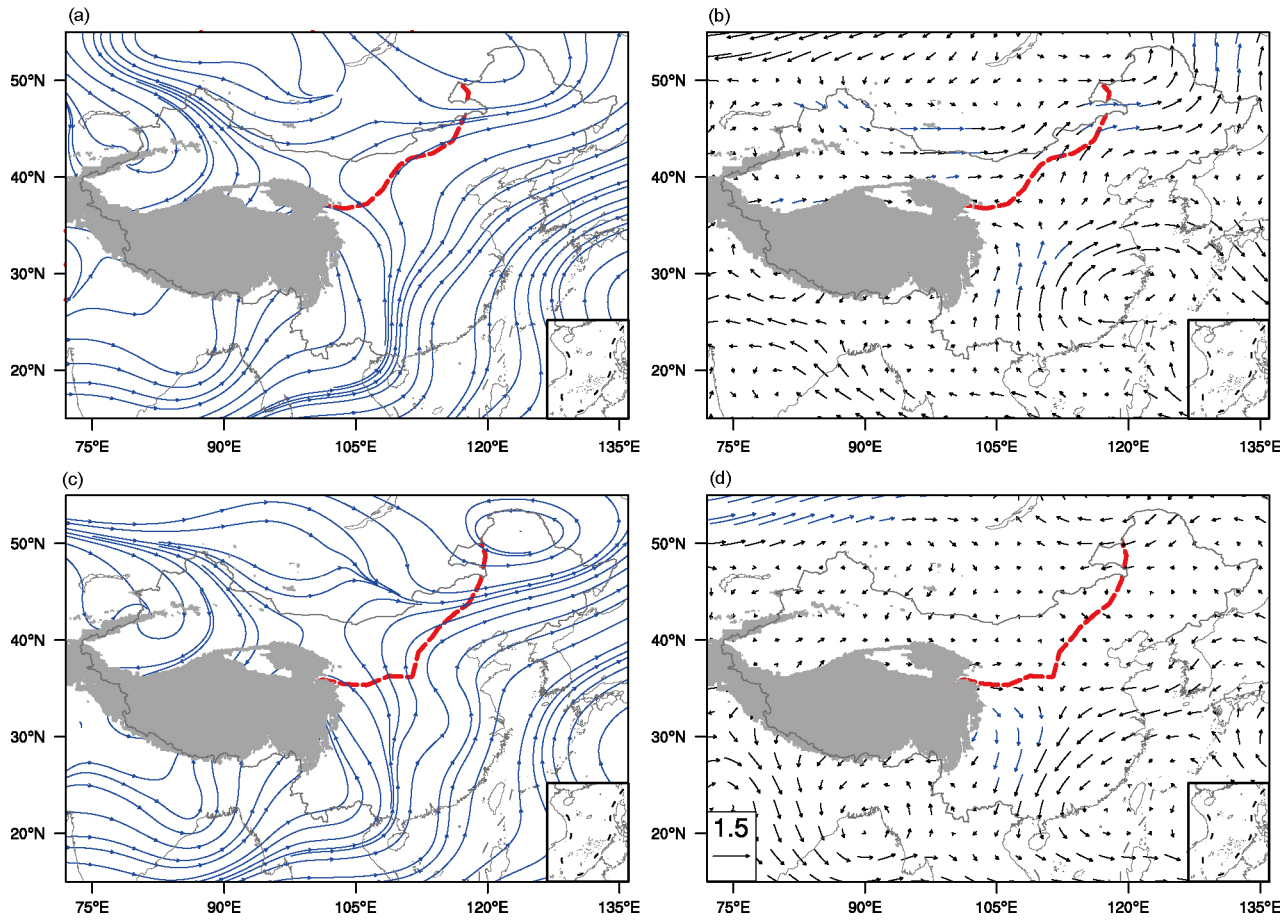

Figure 5 July−August wind vectors at 850 hPa when the locations of the EASM northern boundaries are in northerly-located years (a) and southerly-located years (b), and the composite analysis of the wind vectors in northerly-located years (c) and southerly-located years (d) *versus* climatological (1980−2015) wind vectors. The blue vectors indicate significance at the 90% confident level. The red dashed line shows the locations of the EASM northern boundary.

regions in southerly-located years (Figure 5d).

The foregoing analysis clearly demonstrates that the relationship between the summer monsoon and westerly winds is extremely complex in Northeast China. Figure 5b and d show that both the summer monsoon and the westerly winds are enhanced when the locations of the interannual EASM northern boundaries are more northerly; however, there is no significant change in the westerly winds when the locations are more southerly. The strengthening of the summer monsoon and the westerly winds contribute to the northward location of the cyclone in Northeast China. However, several key issues arise, including the reason why the westerly winds are enhanced when the EASM northern boundaries are in a more northerly location; the nature of the connections between them, and the related mechanisms; whether the westerly winds and the summer monsoon were simultaneously enhanced in the past and whether this will be the case in the future; and whether are there differences on different timescales. These questions clearly need to be addressed in future research.

4. Conclusions and prospects

To study the long-term EASM northern boundary and its spatial variations**,** we have used the concept of the GM to define a new EASM northern boundary index, named the Climatological Northern Boundary Index (CNBI). We then use the CNBI to evaluate interannual spatiotemporal changes in the EASM northern boundary, focusing on the relationship between changes in the boundary and climate, atmospheric circulation, and the distribution of modern land cover and PNV types. Our exploration of the possible mechanisms of changes in the boundary leads to the following conclusions:

(1) The summer (May−September) 2 mm day^{-1} isoline is used to defined the EASM northern boundary index. It reliably depicts the EASM northern boundary in China and reflects the locations of major shifts in wind direction in the summer monsoon circulation. The climatological EASM northern boundary of the CNBI is also consistent with that based on daily precipitation data. It has a clear climatic significance and we propose its use as a new index of the EASM northern boundary.

(2) The climatological EASM northern boundary has a northwest-southwest orientation located along the eastern part of the Qilian Mountains-southern foothills of the Helan Mountains-Daqing Mountains-and the western margin of the Greater Khingan Range, from west to east across Northwest and Northeast China. The interannual changes of the EASM northern boundary cover the central part of Gansu, the northern part of Ningxia, the eastern part of Inner Mongolia and the northeastern region in China. There is a 200−700 km range of fluctuation of the interannual EASM northern boundaries around the locations of the climatological northern boundary. In addition, the spatial fluctuations in the interannual EASM northern boundary gradually increase from west to east, whereas the trend of north-south fluctuations remains roughly constant in different regions.

(3) Using the CNBI, the interannual spatial variations of the EASM northern boundary are approximately located in the region of grasslands and woody savannas, a transitional climate zone and a climatically sensitive zone. The boundary also fluctuates in the region of savanna and grassland according to the PNV types where they are unaffected by human activity. The climatological EASM northern boundary is consistent with the central line between the distribution of grasslands and open shrublands in modern land cover types, located within the area of semi-arid climate, and it also coincides with the major axis of mountain ranges in China. Therefore, the EASM northern boundary has a clear climatic, ecological and geographical significance.

(4) When the locations of the EASM northern boundary are more northerly, the summer monsoon is usually strong, resulting in the increased transport of warm and humid air to the northern part of China; at the same time, the westerly winds are enhanced. The summer monsoon and the westerly winds both contribute to the northward shift of the cyclone in Northeast China. When the locations of the EASM northern boundary are more southerly, the weakening of the EASM reduces the northerly transport of warm and wet air.

It is noteworthy that the interaction between climate change and ecosystems allows mutual verification between the EASM and the distribution of land cover types, and in this study, we used land cover types to verify the CNBI of the EASM. In addition, the fluctuations in the annual EASM northern boundary can also be used to characterize the distribution of land cover types. In recent decades, there has been the increasing availability of accurate land cover data, but in contrast it is difficult to obtain reliable vegetation data for use in paleoecological studies on long timescales, and for future emissions scenarios. Combining changes in the EASM northern boundary on different timescales with the distribution of terrestrial ecosystems can provide a valuable reference for ecosystems study on long timescale, but this aspect of the research needs to be further explored.

Acknowledgements *Thank the two anonymous reviewers for their constructive comments and suggestions. This work was supported by the National Natural Science Foundation of China (Grant Nos. 41505043 & 41372180).*

References

Chen F H, Yu Z H, Yang M L, Ito E, Wang S M, Madsen D B, Huang X Z, Zhao Y, Sato T, Birks H J B, Bommer I, Chen J H, An C B, Wünnemann B. 2008. Holocene moisture evolution in arid central Asia and its out-of-phase relationship with Asian monsoon history. Quat Sci Rev, 27: 351–364

Chen F H, Chen J H, Holmes J, Boomer I, Austin P, Gates J B, Wang N L,

Brooks S J, Zhang J W. 2010. Moisture changes over the last millennium in arid central Asia: A review, synthesis and comparison with monsoon region. Quat Sci Rev, 29: 1055–1068
Chen J, Sun S Q. 1999. Eastern Asian winter monsoon anomaly and variation of global circulation part I: A comparison study on strong and weak winter monsoon (in Chinese). Chin J Atmos Sci, 23: 101–110
Feng S, Fu Q. 2013. Expansion of global drylands under a warming climate. Atmos Chem Phys, 13: 10081–10094
Friedl M A, Strahler A H, Hodges J. 2010. ISLSCP II MODIS (Collection 4) IGBP Land Cover, 2000–2001. In: Forest G, Collatz G, Meeson B, Los S, Brown de Colstoun E, Landis D, eds. ISLSCP Initiative II Collection. Oak Ridge: Oak Ridge National Laboratory Distributed Active Archive Center
Fu C B. 1992. Transitional climate zones and biome boundaries: A case study from China. In: Hansen A J, Castri F D, eds. Landscape Boundaries. New York: Springer-Verlag. 394–402
Fu C B. 2003. Potential impacts of human-induced land cover change on East Asia monsoon. Glob Planet Change, 37: 219–229
Gu L, Wei K, Huang R H. 2008. Severe disaster of blizzard, freezing rain and low temperature in January 2008 in China and its association with the anomalies of East Asian monsoon system (in Chinese). Clim Environ Res, 13: 405–418
Guo Q Y. 1994. Relationship between the variations of East Asian winter monsoon and temperature anomalies in China (in Chinese). Q J Appl Meteor, 5: 218–225
Harris I, Jones P D, Osborn T J, Lister D H. 2014. Updated high-resolution grids of monthly climatic observations—The CRU TS3.10 Dataset. Int J Climatol, 34: 623–642
Hsu P, Li T, Wang B. 2011. Trends in global monsoon area and precipitation over the past 30 years. Geophys Res Lett, 38: L08701
Hu H R, Qian W H. 2007. Identifying the northernmost summer monsoon location in East Asia. Prog Nat Sci, 17: 812–820
Huang R H, Zhou L T, Chen W. 2003. The progresses of recent studies on the variabilities of the East Asian Monsoon and their causes. Adv Atmos Sci, 20: 55–69
Huffman G J, Adler R F, Bolvin D T, Gu G. 2009. Improving the global precipitation record: GPCP Version 2.1. Geophys Res Lett, 36: L17808
Jiang D B, Tian Z P, Lang X M. 2015a. Mid-Holocene global monsoon area and precipitation from PMIP simulations. Clim Dyn, 44: 2493–2512
Jiang D B, Tian Z P, Lang X M, Kageyama M, Ramstein G. 2015b. The concept of global monsoon applied to the last glacial maximum: A multi-model analysis. Quat Sci Rev, 126: 126–139
Jiang J, Jiang D B, Lin Y H. 2015. Monsoon area and precipitation over China for 1961–2009 (in Chinese). Chin J Atmos Sci, 39: 722–730
Jiang Z H, He J H, Li J P, Yang J H, Wang J. 2006. Northerly advancement characteristics of the East Asian Summer Monsoon with its interdecadal variations (in Chinese). Acta Geog Sin, 61: 375–686
Kalnay E, Kanamitsu M, Kistler R, Collins W, Deaven D, Gandin L, Iredell M, Saha S, White G, Woollen J, Zhu Y, Leetmaa A, Reynolds R, Chelliah M, Ebisuzaki W, Higgins W, Janowiak J, Mo K C, Ropelewski C, Wang J, Jenne R, Joseph D. 1996. The NCEP/NCAR 40-year reanalysis project. Bull Amer Meteorol Soc, 77: 437–471
Li D L, Shao P C, Wang H. 2013. The position variations of the north boundary of East Asian subtropical summer monsoon during 1951–2009 (in Chinese). J Desert Res, 33: 1511–1519
Lin R P, Zhou T J, Qian Y. 2014. Evaluation of global monsoon precipitation changes based on five reanalysis datasets. J Clim, 27: 1271–1289
Liu J, Wang B, Ding Q H, Kuang X Y, Soon W, Zorita E. 2009. Centennial variations of the global monsoon precipitation in the last millennium: Results from ECHO-G model. J Clim, 22: 2356–2371
Liu J, Wang B, Yim S Y, Lee J Y, Jhun J G, Ha K J. 2012. What drives the global summer monsoon over the past millennium? Clim Dyn, 39: 1063–1072
Qian W H, Lee D K. 2000. Seasonal march of Asian summer monsoon. Int J Climatol, 20: 1371–1386
Qian W H, Lin X, Zhu Y F, Xu Y, Fu J L. 2007. Climatic regime shift and decadal anomalous events in China. Clim Change, 84: 167–189
Qian W H, Ding T, Hu H R, Lin X, Qin A M. 2009. An overview of dry-wet climate variability among monsoon-westerly regions and the monsoon northernmost marginal active zone in China. Adv Atmos Sci, 26: 630–641
Ramage C S. 1971. Monsoon Meteorology. New York: Academic Press. 1–296
Ramankutty N, Foley J A. 2010. ISLSCP II Potential Natural Vegetation Cover. In: Forest G, Collatz G, Meeson B, Los S, Brown de Colstoun E, Landis D, eds. ISLSCP Initiative II Collection. Oak Ridge: Oak Ridge National Laboratory Distributed Active Archive Center
Schamm K, Ziese M, Raykova K, Becker A, Finger P, Meyer-Christoffer A, Schneider, U. 2015. GPCC Full Data Daily Version 1.0 at 1.0°: Daily Land-Surface Precipitation from Rain-Gauges Built on GTS-based and Historic Data
Shi Z T. 1996. Regional characters of natural disaster in marginal monsoon belt of China (in Chinese). J Arid Land Resour Environ, 10: 1–7
Sun J Q, Wang H J, Yuan W, Chen H P. 2010. Spatial-temporal features of intense snowfall events in China and their possible change. J Geophys Res, 115: D16110
Tang X, Chen B D, Liang P, Qian W H. 2010. Definition and features of the north edge of the East Asian summer monsoon. Acta Meteorol Sin, 24: 43–49
Trenberth K E, Stepaniak D P, Caron J M. 2000. The global monsoon as seen through the divergent atmospheric circulation. J Clim, 13: 3969–3993
Wang A Y, Wu C S, Lin W S, Yang Y, Feng R Q, Gu Z M, Liang J J. 1999. The definition of the advance and retreat of the summer monsoon in China (in Chinese). Plateau Meteor, 18: 400–408
Wang B, Lin B. 2002. Rainy season of the Asian-Pacific summer monsoon. J Clim, 15: 386–398
Wang B, Ding Q. 2006. Changes in global monsoon precipitation over the past 56 years. Geophys Res Lett, 33: L06711
Wang B, Ding Q. 2008. Global monsoon: Dominant mode of annual variation in the tropics. Dyn Atmos Oceans, 44: 165–183
Wang B, Liu J, Kim H J, Webster P J, Yim S Y. 2012. Recent change of the global monsoon precipitation (1979–2008). Clim Dyn, 39: 1123–1135
Wang B, Yim S Y, Lee J Y, Liu J, Ha K J. 2014. Future change of Asian-Australian monsoon under RCP 4.5 anthropogenic warming scenario. Clim Dyn, 42: 83–100
Wang H, Yu E, Yang S. 2011. An exceptionally heavy snowfall in Northeast china: Large-scale circulation anomalies and hindcast of the NCAR WRF model. Meteorol Atmos Phys, 113: 11–25
Wang L, Chen W, Huang G, Zeng G. 2017. Changes of the transitional climate zone in East Asia: Past and future. Clim Dyn, 49: 1463–1477
Wang P X. 2009. Global monsoon in a geological perspective (in Chinese). Chin Sci Bull, 54: 1113–1136
Wang P X, Wang B, Cheng H, Fasullo J, Guo Z T, Kiefer T, Liu Z Y. 2014. The global monsoon across timescales: Coherent variability of regional monsoons. Clim Past, 10: 2007–2052
Webster P J. 1987. Monsoon. In: Wiley J, ed. The Elementary Monsoon. New York: Academic Press. 3–32
Wen M, Yang S, Kumar A, Zhang P Q. 2009. An analysis of the large-scale climate anomalies associated with the snowstorms affecting China in January 2008. Mon Weather Rev, 137: 1111–1131
Winkler M G, Wang P K. 1993. The late Quaternary vegetation and climate of China. In: Wright H E, Kutzbach J E, Webb T, Rudiman W F, Street-Perrott F A, Bartlein P J, Eds. Global Climates since the Last Glacial Maximum. Minneapolis: University of Minnesota Press. 221–261
Wu C G, Liu H S, Xie A. 2005. Interdecadal characteristics of the influence of northward shift and intensity of summer monsoon on precipitation over northern China in summer (in Chinese). Plateau Meteorol, 24: 656–665

Xie P P, Arkin P A. 1997. Global precipitation: A 17-year monthly analysis based on gauge observations, satellite estimates, and numerical model outputs. Bull Amer Meteorol Soc, 78: 2539–2558

Xu Y, Qian W H. 2003. Research on East Asian summer monsoon: A review (in Chinese). Acta Geog Sin, 58: 1–9

Yan G H, Li Q P, Lv D H. 2008. Climate change and future trends of the farming-grazing zone in Northern China (in Chinese). J Nanjing Inst Meteorol, 31: 671–678

Zhao Y X, Qiu G W. 2001. A study of climate change impact on northern farming-pastoral region (in Chinese). Meteorol Monther, 27: 3–7

Zhou T J, Zhang L X, Li H M. 2008a. Changes in global land monsoon area and total rainfall accumulation over the last half century. Geophys Res Lett, 35: L16707

Zhou T J, Yu R C, Li H G, Wang B. 2008b. Ocean forcing to changes in global monsoon precipitation over the recent half-century. J Clim, 21: 3833–3852